

---

## THEORY OF DIRECTION SENSITIVE PROBES FOR ELECTRODIFFUSION MEASUREMENT OF WALL VELOCITY GRADIENTS

Ondřej Wein and Václav SOBOLÍK

*Institute of Chemical Process Fundamentals,  
Czechoslovak Academy of Sciences, 165 02 Prague 6 - Suchbát*

Received December 8th, 1986

---

Theory of segmented circular electrodes for electrodiffusion measurements is developed in the diffusion layer approximation. A fast subroutine is given for handling the data supplied by three-segment circular electrode.

---

Determination of the absolute values of velocity gradients or corresponding shear stresses at a wall by using the electrodiffusion limiting current technique<sup>1,2</sup> belongs to well-developed standard experimental methods. On the contrary, the electrodiffusion measurement of instantaneous flow direction<sup>2-4</sup> presented rather difficult task till this time. To master this task, the following three stages have to be solved:

- a) manufacture of a multi-segment electrode,
- b) reliable calibration method for determining the directional characteristic,
- c) fast transformation of the primary multiple current signal to the information on the flow direction.

In the recent patent<sup>5</sup>, an improved technology is described of manufacturing multi-segment circular electrodes. The technology is applicable for the series production of electrodiffusion probes sensitive to direction of the flow. The calibration experiments<sup>6</sup> with a prototype three-segment electrode have shown its high directional sensitivity as well as the independency of the directional characteristic on the flow rate.

In the present work, the theory is given of electrochemically induced convective diffusion to a segmented circular electrode in a unidirectional velocity field with a constant velocity gradient. The special case of an electrode composed of three identical radial segments is considered in details, including an algorithm for deciphering of the multiple current data.

### THEORETICAL

Primary quantity in any electrodiffusion diagnostics of flow is the limiting current<sup>1,2</sup>. For a given concentration field  $c$  of a species consumed by an electrode reaction,

i.e. depolarizer, the limiting current  $i_A$  is given as the surface integral of the local current densities  $J$  over the electrode surface  $A$ :

$$i_A = \iint_A J \, dA, \quad (1)$$

where the local density  $J$  is expressed by the Faraday law,

$$J = nFD|\nabla c|. \quad (2)$$

In a distance from the electrode surface,  $z = \infty$ , the depolarizer concentration is constant and equal to that in the fresh solution,  $c = c_0$ . Immediately at the electrode surface,  $z = 0$ ,  $(x, y) \in A$ , the concentration is negligible small,  $c = 0$ , due to depletion of the depolarizer by a fast electrode reaction under the condition of limiting diffusion currents<sup>1</sup>.

For the kinematics of flow shown in Fig. 1,  $v_y = 0$ ,  $v_z = 0$ ,  $v_x = qz$ , the equation of steady convective diffusion,

$$\mathbf{v} \cdot \nabla c = D \nabla^2 c, \quad (3)$$

can be reduced to the following form:

$$zq\partial_x c = D(\partial_{zz}^2 c + \partial_{xx}^2 c + \partial_{yy}^2 c). \quad (4)$$

The longitudinal coordinate  $x$  is oriented parallelly to the flow direction and has the origin,  $x = 0$ , at the forward edge of the electrode. The normal coordinate  $z$  is oriented perpendicularly to and has the origin,  $z = 0$ , in the electrode surface. The transversal coordinate  $y$  is orthogonal to both  $x$  and  $z$ , and has arbitrary location of the origin.

The longitudinal and transversal diffusion terms,  $D\partial_{xx}^2 c$  and  $D\partial_{yy}^2 c$  have a perceivable effect only under the condition of extremally low Peclet number<sup>7</sup>,  $qL^2/D < 10^3$ , where  $L = \min(L_x, L_y)$ . The relevant boundary-value problem becomes substantially simpler if both the longitudinal and transversal diffusion terms are neglected in the transport equation (4). The resulting parabolic problem with the local boundary conditions

$$\begin{aligned} c &= c_0: & \text{for } z = \infty & \text{ or } x = 0, \\ c &= 0: & \text{for } z = 0 & \text{ and } x > 0, \end{aligned} \quad (5)$$

can be solved by introducing the well-known similarity transformation,  $c(z, x, y) = c_0 C(w)$ ,  $w = z(9Dx/q)^{-1/3}$ , with the following result:

$$c(x, z) = c_0 \int_0^w \exp(-s^3) ds / \int_0^\infty \exp(-s^3) ds. \quad (6)$$

The corresponding surface field of the local current densities can be written as follows:

$$J = Kx^{-1/3}, \quad (7)$$

where

$$K = nFc_0D^{2/3}(q/9)^{1/3}/\Gamma(4/3). \quad (8)$$

It should be noticed that the longitudinal distance  $x$  of a surface point is measured from the forward edge of the electrode along the corresponding streamline.

The same expression for the local current density  $J$  is valid for any part  $S$  of the ideally polarized electrode  $A$ , which will be called the segment  $S$ . Under the condition of the unidirectional shear flow, the streamlines are both straight and parallel so that the general expression (7) can be written in the following explicit form for any segment  $S \subset A$ :

$$\begin{aligned} i_S &= K \iint_S x^{-1/3} dA = K \int_{y_0}^{y_1} dy \int_{x_0(y)}^{x_1(y)} x^{-1/3} dy = \\ &= \frac{3}{2}K \int_{y_0}^{y_1} ([x_1(y)]^{2/3} - [x_0(y)]^{2/3}) dy, \end{aligned} \quad (9)$$

see also Fig. 2.

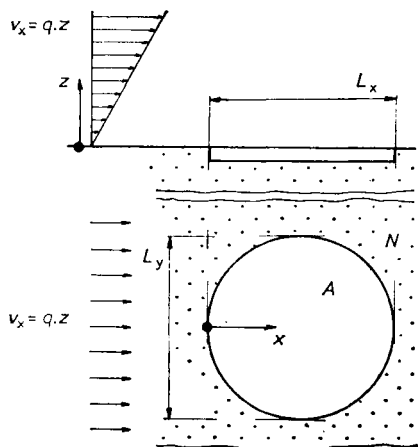


FIG. 1  
Circular electrode for shear rate measurements

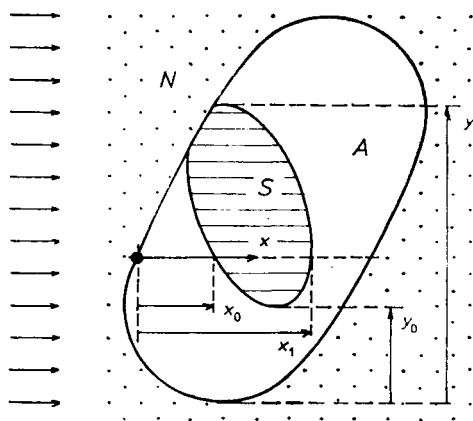


FIG. 2  
General schema of segmented electrode

### Current through a Radial Segment

Geometry of any radial segment of a given circular electrode is unambiguously specified by a single parameter, *e.g.* the half-angle  $a$ , see Fig. 3. The orientation of the segment relative to the flow direction can be specified *e.g.* by the angle  $t$ . However, it is advantageous to introduce the alternate pair of geometric parameters,

$$b_1 = t - a, \quad b_2 = t + a, \quad (10)$$

for computation of the current  $i_s$  through the segment. The constraint  $0 < b_2 - b_1 < 2\pi$  expresses the obvious fact that the condition  $0 < a < \pi$  should hold for any real segment.

The total current through a circular electrode  $A$ , *i.e.* for  $b_2 = b_1 + 2\pi$ , is given by the following well-known formula<sup>1-3</sup>:

$$i_A = \frac{2}{3} K (2R)^{5/3} 2 \int_0^1 (1-t^2)^{1/3} dt = 2 \cdot 15695 n F c_0 D^{2/3} R^{5/3} q^{1/3}. \quad (11)$$

The ratio  $I_S = i_s/i_A$  for a radial segment depends only on angles  $(b_1, b_2)$  or  $(t, a)$ :

$$I_S = H(b_1, b_2) = H(t - a, t + a). \quad (12)$$

Eight different subdomains of the arguments  $(b_1, b_2)$  of the function  $H$  should be

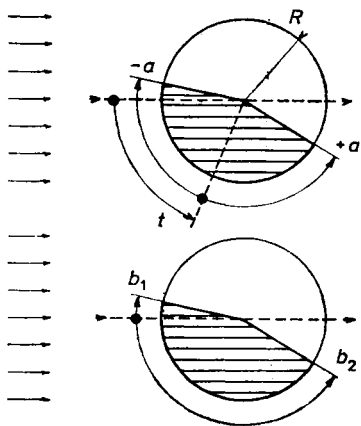


FIG. 3  
Circular electrode with radial segment

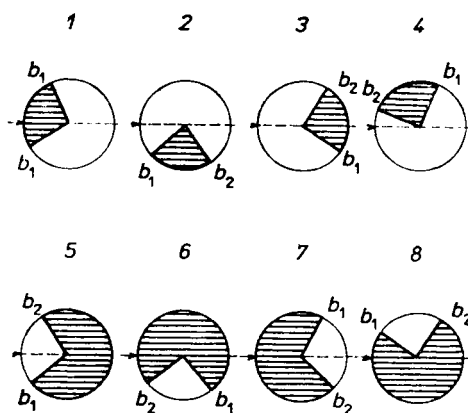


FIG. 4  
Eight possible configurations of single radial segment

distinguished in actual computations of  $H$ -values by means of the general formula (9). The individual cases are shown in Fig. 4. The computations can be simplified considerably by using the following functional rules:

$$\begin{aligned} H(b, b + 2\pi) &= 1, \\ H(b_1, b) + H(b, b_2) &= H(b_1, b_2), \\ H(2\pi - b_2, 2\pi - b_1) &= H(b_1, b_2), \end{aligned} \quad (13)$$

which follow from the obvious properties of the set function  $I_S = I(S)$ ,  $S \subset A$ . These rules make possible to express the function  $H$  of two independent arguments  $(b_1, b_2)$  through another function  $F^*$  of a single argument:

$$F^*(b) = H(0, b); \quad 0 < b < \pi. \quad (14)$$

The corresponding composite rules, which are listed in Table I, can be unified to the following single expression for  $H$ :

$$H(b_1, b_2) = F(b_2) - F(b_1). \quad (15)$$

The function  $F$  of the single argument,  $b \in (-\infty; +\infty)$ , represents an extension of the original function  $F^*$ , as defined by the following symmetry rules:

$$\begin{aligned} 0 < b < \pi: \quad F(b) &= F^*(b), \\ \pi < b < 2\pi: \quad F(b) &= 1 - F^*(2\pi - b), \end{aligned}$$

TABLE I

Rules for computation of  $H(b_1, b_2)$  on eight different subdomains

Case <sup>a</sup>	Conditions <sup>b</sup>	Representation of $H(b_1, b_2)$
1	$-\pi < b_1 < 0 < b_2 < \pi$	$F^*(b_2) + F^*(-b_1)$
2	$0 < b_1 < 0 < b_2 < \pi$	$F^*(b_2) - F^*(b_1)$
3	$0 < b_1 < \pi < b_2 < 2\pi$	$1 - F^*(2\pi - b_2) - F^*(b_1)$
4	$\pi < b_1 < b_2 < 2\pi$	$-F^*(2\pi - b_2) + F^*(2\pi - b_1)$
5	$-2\pi < b_1 < -\pi < b_2 < 0$	$1 - F^*(-b_2) - F^*(2\pi + b_1)$
6	$-2\pi < b_1 < 0 < b_2 < \pi$	$1 + F^*(b_2) - F^*(2\pi + b_1)$
7	$-\pi < b_1 < 0 < b_2 < \pi$	$F^*(-b_1) + F^*(b_2)$
8	$-\pi < b_1 < 0 < \pi < b_2$	$1 + F^*(2\pi - b_2) + F^*(-b_1)$

<sup>a</sup> See also Fig. 4; <sup>b</sup> the condition  $b_2 - b_1 < 2\pi$  is implicitly assumed.

$$\begin{aligned}
 -\pi < b < 0: & \quad F(b) = -F^*(-b), \\
 -2\pi < b < -\pi: & \quad F(b) = -1 + F^*(2\pi + b), \\
 -\infty < b < +\infty: & \quad F(b) = F(4\pi + b).
 \end{aligned} \tag{16}$$

The function  $F^*(b)$  was determined by numerical integration. Two subcases have been considered which correspond to  $b < \pi/2$  and  $\pi/2 < b$ , respectively, see Fig. 5. From obvious geometrical consideration, the following two expressions hold for the lengths of streamlines crossing the segment territory:

$$x_1(y) = \begin{cases} (R^2 - y^2)^{1/2} - y \cotg b; & 0 < y < y_s \\ 2(R^2 - y^2)^{1/2}; & y_s < y < R, \end{cases} \tag{17}$$

where  $y_s = R \sin b$  and  $x_0(y) = 0$  for any convex segment,  $b < \pi$ . The starting expression for  $i_s$ ,

$$i_s = \begin{cases} \frac{3}{2}K \int_0^{y_s} [x_1(y)]^{2/3} dy; & b < \pi/2 \\ \frac{3}{2}K \left\{ \int_0^{y_s} + \int_{y_s}^R \right\} [x_1(y)]^{2/3} dy; & b > \pi/2, \end{cases} \tag{18}$$

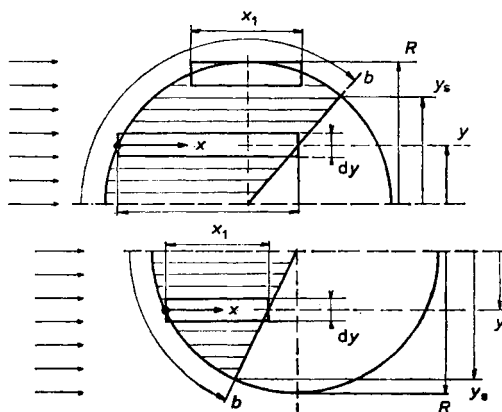


FIG. 5

Integration schema for two basic kinds of radial segments,  $b < \pi/2$  and  $\pi/2 < b$

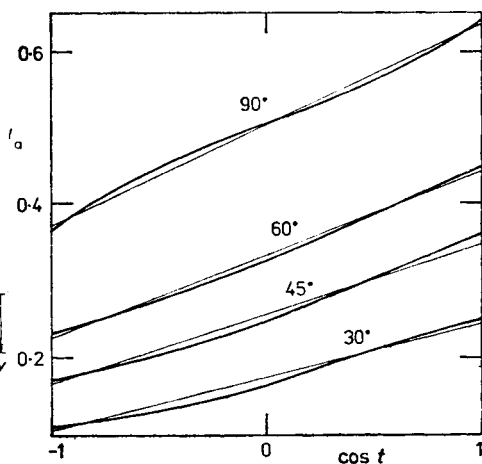


FIG. 6

Directional characteristics for single radial segments. Numerical labels give  $\alpha$ -values in the  $360^\circ$ -scale

can be converted by some manipulations to the following analytic formula for  $F(b) = I_S$ :

$$F(b) = \begin{cases} \frac{S}{P} \int_0^1 [w - Ct]^{2/3} dt; & b < \pi/2 \\ \frac{1}{2} - \frac{S}{P} \int_0^1 ([2w]^{2/3} - [w - Ct]^{2/3}) dt; & b > \pi/2, \end{cases} \quad (19)$$

where

$$S = \sin b, \quad C = \cos b, \quad w = (1 - S^2 t^2)^{1/2},$$

$$P = 2^{5/3} \int_0^1 [1 - t^2]^{1/3} dt = 2.670984369. \quad (20)$$

#### *Directional Characteristics of Individual Segments*

For a given radial segment  $S$ , specified by the radius  $R$  and half-angle  $a$ , the dependence of the normalized current  $I_S$  on the segment orientation  $t$  (or the flow direction  $-t$ ) is expressed by the function

$$I_a(t) = H(t - a, t + a). \quad (21)$$

For several values of the half-angle  $a$ , this function is shown in Fig. 6. The argument  $\cos(t)$  is used there instead of  $t$  to demonstrate that the functions  $I_a(t)$  can be represented well by the simple empirical formulas  $I_a(t) = B_0(a) + B_1(a) \cos(t)$ . More exactly, the Fourier series of the functions  $I_a(t)$ :

$$I_a(t) = B_0(a) + \sum_{m=1}^{\infty} B_m(a) \cos(mt). \quad (22)$$

will undoubtedly converge very fast. The numerical realisation of the corresponding Fourier coefficients,

$$B_0(a) = \frac{1}{\pi} \int_0^{\pi} I_a(t) dt, \quad (23)$$

$$B_m(a) = \frac{2}{\pi} \int_0^{\pi} I_a(t) \cos(mt) dt, \quad (24)$$

resulted in the following simple expressions:

$$B_0(a) = a/\pi, \quad B_m(a) = C_m \sin(ma), \quad (25)$$

which certainly have an exact analytical background. The numerical values of  $C_m$  are given in Table II. The reduced approximate formula

$$I_a(t) = a/\pi + 0.126 \sin a \cos t + 0.007 \sin 2a \cos 2t \quad (26)$$

guarantees the accuracy better than  $\pm 0.005$  over the whole region of the parameters  $(a, t)$ .

## RESULTS AND DISCUSSION

### *Directional Characteristic of Three-Segment Circular Electrode*

In the present paragraph, the current signal is considered of a circular electrode which consists of three mutually isolated, but equally polarized and geometrically identical radial segments,  $j = 1, 2, 3$ . The directional characteristic of such a multiple electrode system is presented by a triplet of functions  $I_j(t)$  expressing the current-direction dependencies of the individual segments, see Fig. 7. The definition of the  $t$ -variable is common for all the segments. For the case under consideration, the functions  $I_j(t)$  can be expressed in the following way:

$$I_j(t) = I_a(t - t_0 - 2\pi j/3), \quad (27)$$

where the  $t_0$ -value depends on the optional setting the zero direction for the electrode as a whole.

If the individual characteristics can be represented by formulas like Eq. (26), then the entire characteristic of a real three-segment electrode is represented by the matrix  $B_{jm}$ ,  $m = 0, \dots, 4$ , of the Fourier coefficients for individual segments:

$$I_j(t) = B_{j0} + B_{j1} \sin t + B_{j2} \cos t + B_{j3} \sin 2t + B_{j4} \cos 2t. \quad (28)$$

TABLE II  
Universal coefficients of directional characteristics represented by the Fourier series

$m$	$C_m$	$m$	$C_m$
1	+0.12613828	5	+0.00050387
2	+0.00701656	6	+0.00015206
3	-0.00302874	7	-0.00015117
4	-0.00064083		



The shifts of the axes of individual segments,  $j = 1, \dots, 3$ , cause the appearance of sin-terms in these expressions.

### How to Treat Signals from Real Three-Segment Electrode

Normalized current signal is represented by a triplet of the values  $[I_j^+]$ ,  $j = 1, \dots, 3$ . Obviously, the corresponding information is redundant in certain sense, because only a single value – the direction angle  $t$  – should be determined by solving the system of three nonlinear equations

$$I_j(t) - I_j^+ = 0; \quad j = 1, 2, 3, \quad (29)$$

with the additional constraints

$$I_1(t) + I_2(t) + I_3(t) = 1, \quad I_1^+ + I_2^+ + I_3^+ = 1. \quad (30)$$

Common ways of treating such non-linear systems<sup>8</sup> result in rather slow computational processes which are unsuitable for on-line treating of large sets of primary current data.

Fortunately, there exists an extremely effective way for solving the system of Eqs (29) and (30) in the case under consideration. It is based on the fact that the conditions

$$I_p^+ < I_q^+ < I_r^+, \quad (31)$$

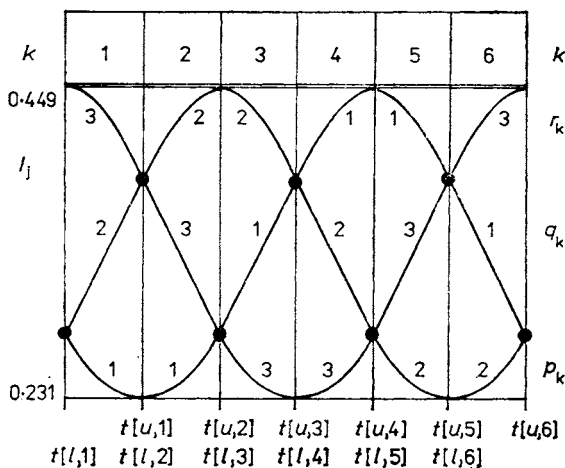


FIG. 7

Directional characteristic of the circular electrode for the ideal case of three equal segments

can be fulfilled for only one permutation  $[p, q, r]$  of the indexes  $j = 1, 2, 3$ . Obviously, the six sectors,  $k = 1, \dots, 6$ , exist on the interval  $0 < t < 2\pi$ , which are uniquely assigned to the corresponding permutations  $[p, q, r]$ , see Fig. 7. In the  $k$ -th sector, two pairs of values,  $\{t[l, k], I[l, k]\}$  and  $\{t[u, k], I[u, k]\}$ , give the angle and current coordinates of the bounding points, laying on  $I_q(t)$ ,

$$I[l, k] = I_q(t[l, k]), \quad I[u, k] = I_q(t[u, k]). \quad (32)$$

Here, the index  $q = q_k$  and the functions  $I_j(t)$ ,  $j = 1, 2, 3$ , are assumed to be known for the  $k$ -th sector. Having the proper sector identified and  $q = q_k$  known, the single equation

$$I_q(t) - I_q^+ = 0 \quad (33)$$

should be solved for determining the  $t$ -value. Even the linear approximation of the function  $I_q(t)$  inside the  $k$ -th sector,

$$I_q(t) = I[l, k] + (I[u, k] - I[l, k]) \frac{t - t[l, k]}{t[u, k] - t[l, k]} \quad (34)$$

guarantees an acceptable accuracy ( $\pm 2^\circ$ ) of the determination of the angle  $t$ . The PASCAL version of the algorithm described above is given in the Appendix.

On a computer Commodore PC-10 equipped by the 8087 arithmetic coprocessor, the array of 300 triplets  $[I_1^+, I_2^+, I_3^+]$  can be converted to the corresponding  $t$ -values in less than a second. The computational process is slowed down no more than twice if the *regula-falsi* algorithm for the exact determination of  $t$  is included into the FASTANGLE function. In on-line arrangement, the use of this function allows to attain sampling frequency about 200 Hz.

The presented approach neglects unsteady phenomena within the diffusion layer. However, such approach seems to be acceptable in most hydrodynamic measurements because the inertia of commonly used electrodes<sup>1,2</sup> is negligible even under turbulent flow regimes. The problems of correcting the current-time electrodiffusion data on the inertia effects<sup>9</sup> are out of the scope of the present work.

*The authors are grateful to the Alexander von Humboldt Foundation, Bonn (F.R.G.) for the liberal donation of the computer (Commodore PC-10).*

#### LIST OF SYMBOLS

$a$	half-angle of radial segment, see Fig. 3
$A$	surface of area of electrode
$B_{jm}$	Fourier coefficients for $j$ -th segment
$B_m$	Fourier coefficients for ideal single segment
$b_1, b_2$	auxiliary angle parameters, see Eq. (2)

$C_m$	universal constants to the problem
$c, c_0$	depolarizer concentration and its bulk value
$D$	coefficient of diffusion
$nF$	Faraday constant with stoichiometric coefficient
$F, F^*, H$	functions defined by Eqs (13), (15), (11)
$i_A, i_S$	currents through the surfaces $A, S$
$I$	currents normalized by total current, $I = i/i_A$
$I_a(t)$	directional characteristic for single segment
$I_j(t)$	$j$ -th component of directional characteristic for multi-segment electrode
$I_j^+$	actual (measured) values of $I_j(t)$
$I[l, k], I[u, k]$	lower and upper values of $I$ in $k$ -th sector
$J$	local current density
$K$	coefficient defined by Eq. (7)
$L_x, L_y$	longitudinal and transversal dimensions of electrode
$N$	electroinsulating neighbourhood of electrode
$[p, q, r]$	permutation of the indexes 1, 2, 3
$[p_k, q_k, r_k]$	the permutation of the indexes 1, 2, 3 for $k$ -th sector
$q$	wall shear rate, <i>i.e.</i> the absolute value of velocity gradient at wall
$R$	radius of circular electrode
$S$	surface or area of electrode segment
$t$	angle characterizing electrode orientation or flow direction, see Fig. 3
$t[l, k], t[u, k]$	bounds of $k$ -th sector, see Fig. 7
$x_1$	length of streamline on segment territory, see Fig. 5
$y_s$	critical point of radial segment, see Fig. 5
$v$	velocity field

## REFERENCES

1. Hanratty T. J., Campbell J. A. in the book: *Fluid Mechanics Measurements* (R. J. Goldstein, Ed.), p. 559. Hemisphere, Washington 1983.
2. Nakoryakov V. E., Kashinsky O. N., Kozmenko B. K. in the book: *Measuring Techniques in Gas-Liquid Flows* (J. M. Delhay and G. Cognet, Eds), p. 695. Springer, Heidelberg 1984.
3. Py B.: *Int. J. Heat Mass Transfer* 16, 129 (1973).
4. Wichterle K., Žák L.: *Czech. AO* 231308.
5. Sobolík V., Mitschka P., Menzel Th.: *Czech PV* 7278 86.
6. Menzel Th., Sobolík V., Wein O., Onken U.: *Chem.-Ing.-Tech.* 59, 492 (1987)..
7. Wein O., Kovalevskaya N. D.: *Collect. Czech. Chem. Commun.* 52, 634 (1987).
8. Kuester J. L., Mize J. H.: *Optimization Techniques with FORTRAN*. McGraw Hill, Maidenhead 1973.
9. Sobolík V., Wein O., Čermák J.: *Collect. Czech. Chem. Commun.* 52, 913 (1987).

Translated by the author (O.W.).

## APPENDIX

The following function *FASTANGLE* (in PASCAL) can be recommended for the fast computation of directional angles  $t$  from given triplets  $[I_1, I_2, I_3]$  of normalized currents, see Fig. 7 and Eq. (35).

```
function FASTANGLE (I1, I2, I3: real): real;  
var k: integer; I: real;  
begin  
  if I1 <= I2 then if I2 < I3 then begin k := 1; I := I2 end  
    else if I1 < I3 then begin k := 2; I := I3 end  
      else begin k := 3; I := I1 end  
    else if I3 < I2 then begin k := 4; I := I2 end  
      else if I3 < I1 then begin k := 5; I := I3 end  
        else begin k := 6; I := I1 end  
    FASTANGLE := t[u, k] + (t[l, k] - t[u, k]) * (I - I[u, k]) / (I[l, k] - I[u, k])  
end; (* of FASTANGLE*)
```

The only necessary calibration data are  $I, t$  coordinates of the points of intersections of  $I = I(t)$  calibration curves for the individual segments.